Research Article Vol. 6, No. 4 / April 2019 / Optica 436

Lamb-dip spectroscopy of buffer-gas-cooled molecules

V. Di Sarno,[1,2] R. Aiello,[1,2] M. De Rosa,[1,2] I. Ricciardi,[1,2] S. Mosca,[1] G. Notariale,[1] P. De Natale,[3,4] L. Santamaria,[5] and P. Maddaloni[1,2,*]

[1]CNR-INO, Istituto Nazionale di Ottica, Via Campi Flegrei 34, 80078 Pozzuoli, Italy
[2]INFN, Istituto Nazionale di Fisica Nucleare, Sez. di Napoli, Complesso Universitario di M.S. Angelo, Via Cintia, 80126 Napoli, Italy
[3]CNR-INO, Istituto Nazionale di Ottica, Largo E. Fermi 6, 50125 Firenze, Italy
[4]INFN, Istituto Nazionale di Fisica Nucleare, Sez. di Firenze, Via G. Sansone 1, 50019 Sesto Fiorentino, Italy
[5]ASI, Agenzia Spaziale Italiana, Contrada Terlecchia, 75100 Matera, Italy
*Corresponding author: pasquale.maddaloni@ino.cnr.it

Received 28 November 2018; revised 28 February 2019; accepted 1 March 2019 (Doc. ID 353012); published 4 April 2019

Nowadays, buffer-gas cooling represents an invaluable option to produce cold stable molecules, both in view of secondary cooling/trapping strategies towards the achievement of quantum degeneracy and for fundamental studies of complex molecules. From this follows a demand to establish a pool of specialized, increasingly precise spectroscopic interrogation techniques. Here, we demonstrate a general approach to Lamb-dip ro-vibrational spectroscopy of buffer-gas-cooled molecules. The saturation intensity of the selected molecular transition is achieved by coupling the probe laser to a high-finesse optical cavity surrounding the cold sample. A cavity ring-down technique is then implemented to perform saturation sub-Doppler measurements as the buffer (He) and molecular gas flux are varied. As an example, the $(\nu_1 + \nu_3)$ R(1) ro-vibrational line in a 20 Kelvin acetylene sample is addressed. By referencing the probe laser to a Rb/GPS clock, the corresponding line-center frequency as well as the self and foreign (i.e., due to the buffer gas) collisional broadening coefficients are absolutely determined. Our approach represents an important step towards the development of a novel method to perform ultra-precise ro-vibrational spectroscopy on an extremely wide range of cold molecules. In this respect, we finally discuss a number of relevant upgrades underway in the experimental setup to considerably improve the ultimate spectroscopic performance.

https://doi.org/10.1364/OPTICA.6.000436

1. INTRODUCTION

Recent advances in the field of continuous-wave (CW) and femtosecond laser sources have triggered a new series of tabletop-scale spectroscopic experiments able to investigate fundamental physical phenomena with unprecedented accuracy [1]. Thanks to the enhanced interrogation time obtainable with ultracold samples, spectroscopic frequency measurements on atoms and atomic ions have already reached fractional accuracies of parts in 10^{18} and are at the heart of the very best clocks in the world, magnetometers, gyroscopes, and gravimeters [2]. Conversely, as a consequence of their richer internal structure, which makes cooling and detection more complicated than in atoms, molecules are still lagging behind with regard to precision spectroscopic studies. Yet, these extra degrees of freedom in molecules, combined with a charge distribution different than in atomic systems, have the potential to unveil new physics [3]. Examples include: testing quantum electrodynamics with higher levels of precision (proton radius *puzzle* [4], fifth-force interactions [5], proton mass determination [6]), detecting axion dark matter [7,8], assessing the space-time stability of fundamental constants [9,10], and searching for time-reversal violation (an electron's electric dipole moment) [11]. In this framework, worldwide efforts are being made to produce increasingly colder molecular samples, with some experiments working towards quantum degeneracy [12,13]. Nowadays, buffer-gas cooling (BGC) [14,15], first demonstrated by the group of F. C. De Lucia under the name of collisional cooling [16], represents an essential technology for producing low-temperature stable molecules, both as a starting point for secondary cooling/trapping strategies and for a spectroscopic interrogation. Indeed, precision laser spectroscopy has already been applied to buffer-gas-cooled samples in different configurations, both for neutral molecules [17–23] and for molecular ions [24,25]. In this scope, BGC promises to overtake the wealth of high-resolution spectroscopic results obtained to date by the earlier technology of supersonic beams [26–28], provided that dedicated schemes for saturation sub-Doppler spectroscopy are established.

In this work, based on a saturated-absorption cavity ring-down (SCAR) technique [29–32], we demonstrate a general approach to Lamb-dip ro-vibrational spectroscopy of buffer-gas-cooled molecules. Our scheme offers two main benefits: first, cooling

internal degrees of freedom provides a high level of state selectivity, with larger populations in the molecular states of interest; second, cooling the translational motion allows long interaction times and hence reduced transit-time broadening effects. As an example, we use the acetylene molecule (C_2H_2), the subject of several high-resolution spectroscopic studies motivated by the demand for improved frequency standards in the telecommunications range [33–35]. By referencing the probe laser to a Rb/GPS clock via an optical frequency comb synthesizer (OFCS), the Lamb-dip signals corresponding to the $(\nu_1 + \nu_3)$ R(1) rovibrational line are recorded as a function of the flux into the cell of either the buffer gas or the molecules ($\mathcal{F}_{He}$ and $\mathcal{F}_{mol}$). The obtained sub-Doppler profiles are then fitted with a Lorentzian line shape. This enables absolute determination of the line-center frequency as well as of the self and foreign collisional broadening coefficients. At best, the statistical uncertainty on the line-center frequency is as low as 12 kHz ($6 \cdot 10^{-11}$ in fractional terms), while the full width at half-maximum (FWHM) is about 800 kHz. Our method opens the low-temperature range to accurate measurements of basic spectroscopic parameters in gas-phase molecular samples, potentially applicable to a vast range of species.

2. EXPERIMENTAL SETUP

Figure 1 shows the basic components of the combined SCAR spectrometer and BGC apparatus. Described in detail in a previous paper [36], the heart of the BGC machine is represented by a two-stage pulse tube (PT) cryo-cooler (Cryomech, PT415) housed in a stainless-steel vacuum chamber and fed with liquid helium by a compressor. The first (second) PT stage yields a temperature of 45 K (4.2 K) provided that its heat load is kept below 40 W (1.5 W); for this purpose, each plate is enclosed in a gold-plated copper shield (equipped with optical access to allow the laser beam propagation), in order to block sufficient black-body radiation. A single stainless-steel pipe, thermally insulated from both the PT stages, is used to inject both acetylene and helium, contained in room-temperature bottles, into a cubic copper cell of side length $d = 40$ mm (buffer cell), which is in contact with the second PT plate. For each of the two injected gases, capillary filling is regulated upstream by a flow controller with an accuracy of 0.05 SCCM (1 SCCM $= 4.5 \cdot 10^{17}$ molec/s). In this configuration, C_2H_2 molecules are quickly cooled down to 20 K through multiple collisions with the He buffer gas. It is worth remarking that, in a previous work [36], we obtained temperatures around 10 K for the molecular species, as we used a different injection pipeline for the He gas. This comprised, in particular, two spool-shaped copper tubes secured to the 45 K and the 4.2 K plate, respectively. In the present experiment, due to cracks in the weldings of this dedicated buffer-gas pipeline, as already mentioned, a single pipe is used to inject both acetylene and helium. In this way, the buffer gas cools only after entering the cell without exploiting all the available cooling power. The buffer cell is equipped with two opposite circular holes (5 mm diameter), which are aligned along the axis of the spectroscopic enhancement cavity. The latter consists of two facing high-reflectivity (99.995%) spherical mirrors (3 m radius of curvature, 1 inch diameter), at a distance $D = 65$ cm. To ensure an adequate degree of mechanical stability and reliability, specially developed mirror mounts are used (see Fig. 2). Each mount consists of two main parts: (1) a plate against which the mirror and the annular piezoelectric actuator (only for the input mirror) are held thanks to the compression provided by a ring nut (with an interposed o-ring); (2) a system of three manual magnetically coupled micro-rotators that, acting on the micrometric screws mounted on the plate, allow orientation while guaranteeing the vacuum seal. The probe light source is a CW external-cavity diode laser (Toptica Photonics, DLC CTL 1520) delivering about 30 mW of power between 1470 and 1570 nm with a free-running emission linewidth less than 50 kHz at 5 ms. The laser output beam is split into two main parts [37]. One portion is beaten against the Nth tooth of an OFCS (Menlo Systems, FC-1500-250-WG) to provide a note that is then phase-locked to a given local-oscillator

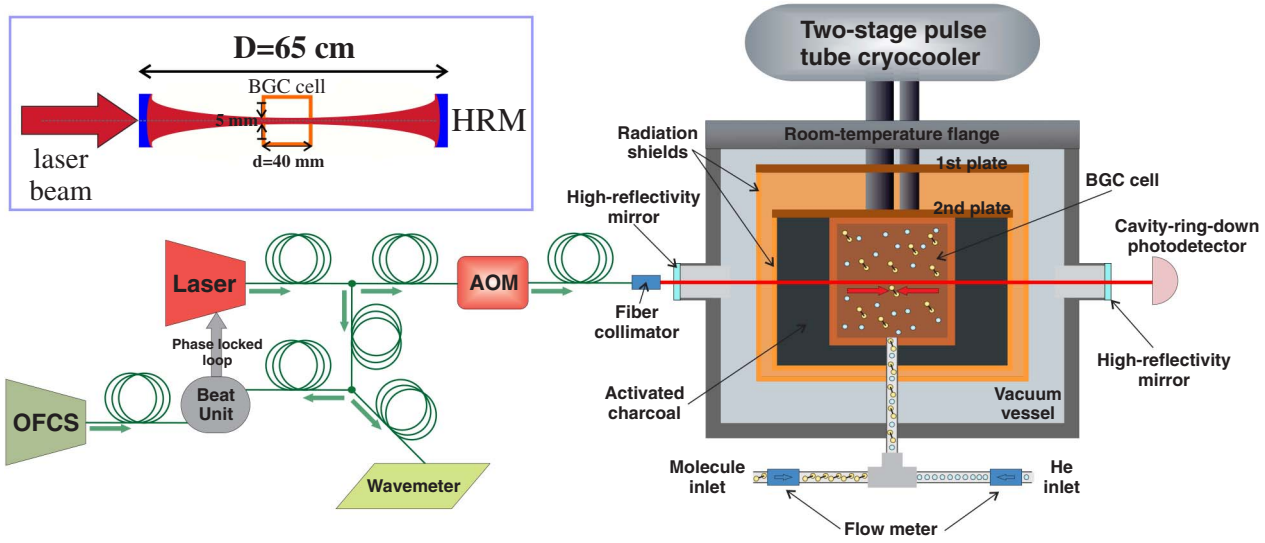

Fig. 1. Schematic layout (not to scale) of the experimental apparatus consisting of two main blocks: the BGC source and the OFCS-referenced probe laser. To keep the pressure inside the radiation shields below 10^{-7} mbar, the internal surface of the inner shield (roughly 1500 cm^2) is covered with a layer of activated charcoal that, at cryogenic temperatures, acts as a pump (with a speed of a few thousands dm^3/s [15]) for helium and non-guided molecules. The gas adsorbed by the charcoal is released during the warm-up of the cryogenic system and then pumped out of the vessel by a turbomolecular pump (not shown). Relevant dimensions of the enhancement cavity and the buffer cell are given in the inset.

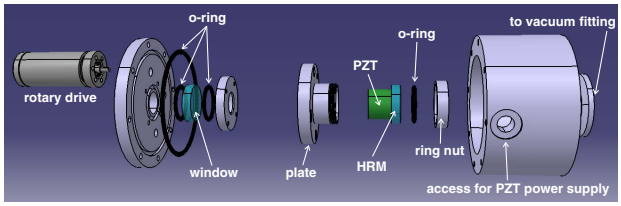

Fig. 2. Exploded sketch of the specially designed cavity mirror mount.

value ($\nu_{LO} \simeq 30$ MHz) by a dedicated electronic servo (Toptica Photonics, mFALC 110). The second portion passes through a fiber acousto-optic modulator (AOM) whose first-diffracted order is injected into the high-finesse cavity to perform SCAR spectroscopy. In this configuration, the laser emission frequency is given by

$$\nu = \nu_{ceo} + N\nu_r + \nu_{LO} + \nu_{AOM}, \quad (1)$$

where ν_{AOM} (80 MHz) is the frequency of the signal driving the AOM, while ν_{ceo} (20 MHz) and ν_r (250 MHz) denote the comb carrier-envelope offset and mode spacing, respectively. The link to the Cs-clock standard is established by stabilizing both ν_{ceo} and ν_r against a high-quality quartz oscillator, which is disciplined, in turn, by a Rb/GPS clock. Such a frequency chain ensures an accuracy of 10^{-13} and a fractional stability (Allan deviation) between $4 \cdot 10^{-13}$ and $8 \cdot 10^{-13}$ for an integration time between 10 and 1000 s. The same chain is used to lock the time base of the frequency synthesizers generating the signals at ν_{LO} and ν_{AOM}, respectively. After determining the integer N by a 0.2-ppm-accuracy wavelength meter, the absolute frequency of the probe laser is monitored by simultaneously counting the frequencies ν_{ceo}, ν_r, and ν_{LO}. Tuning of ν across the Lamb-dip molecular profile is then accomplished by varying ν_{LO} in discrete steps. The length of the optical resonator is continuously dithered by the annular piezoelectric actuator. As a resonance builds up, a threshold detector triggers an abrupt switch-off of the AOM. The subsequent ring-down decay is collected by a transimpedance amplified InGaAs photodetector (5 MHz electrical bandwidth). The average of 60 acquisitions, recorded by a standard 8-bit oscilloscope, is then fitted by a simple exponential decay to yield the corresponding ring-down time $\tau(\nu)$. The absorption coefficient is eventually recovered through the relation

$$\alpha(\nu) = \frac{1}{c}\left[\frac{1}{\tau(\nu)} - \frac{1}{\tau_0}\right]\frac{D}{d}, \quad (2)$$

where $\tau_0 \simeq 45$ μs is the empty-cavity decay constant and c the speed of light.

3. RESULTS AND DISCUSSION

To establish optimal working conditions, a Doppler-limited spectrum is initially acquired; its width, $\sigma_D = (\nu_0/c)\sqrt{8 \ln 2\, m^{-1} k_B T}$, extracted by a fit with a Gaussian profile, returns the temperature T of the molecular sample (here, m is the molecular mass, k_B the Boltzmann constant, and ν_0 the line-center frequency of the selected ro-vibrational transition). As an example, Fig. 3 shows the spectroscopic absorption signal obtained for $\mathcal{F}_{mol} = \mathcal{F}_{He} = 6$ SCCM, corresponding to $T = (20 \pm 3)$ K. It should be noted that equal flows of the two gases do not correspond to equal densities in the buffer cell. In fact, many of the acetylene molecules

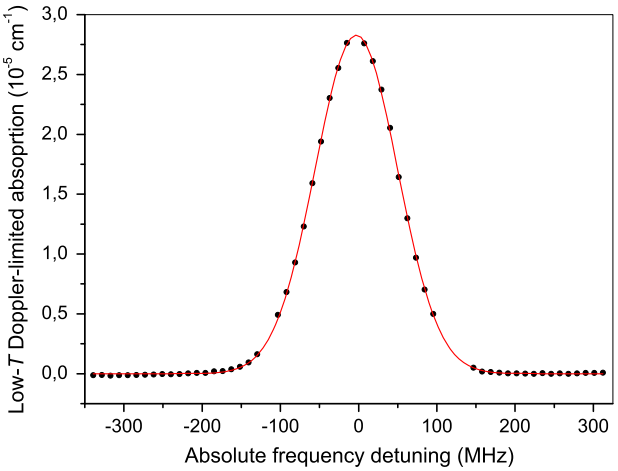

Fig. 3. Doppler-limited spectrum of the $(\nu_1 + \nu_3)$ R(1) ro-vibrational transition of acetylene, obtained for $\mathcal{F}_{mol} = \mathcal{F}_{He} = 6$ SCCM. Fitting with a Gaussian profile yields a temperature of (20 ± 3) K for the C_2H_2 sample. To make the abscissa axis easy to read, rather than ν, the absolute frequency detuning $\nu - \nu_0$ is reported, where ν_0 is the center-frequency value previously measured in [38].

freeze upon impact on the walls; this is not the case for the helium. Nonetheless, after a short transient (less than 10 ms in the worst case), stationary gas densities will be established inside the buffer cell, leading to steady-state spectroscopic absorption profiles. Afterwards, a denser frequency scan is performed around the center of the absorption profile to record the Lamb-dip spectrum. The sub-Doppler feature shown in Fig. 4 is the average over 30 single Lamb-dip acquisitions, each lasting about 30 s for a total measurement time of 900 s (i.e., our maximum allowed integration time, limited by drifts in the cavity decay time). The obtained signal-to-noise ratio is SNR ≃ 30, essentially limited by the residual mechanical noise introduced by the PT cryo-cooler on the cavity mirrors. Then, fitting the dip profile with a

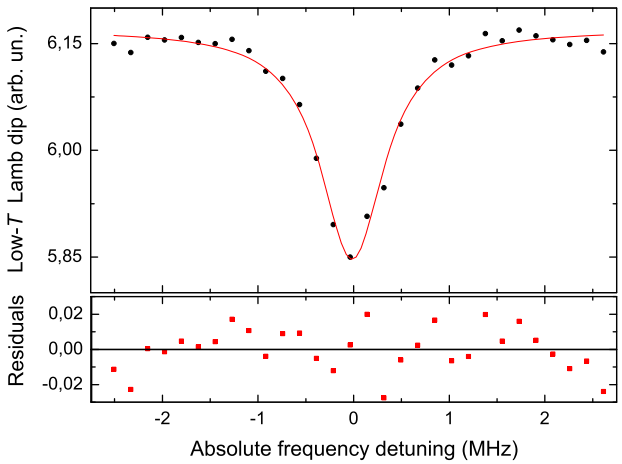

Fig. 4. Lamb-dip line shape corresponding to the Doppler-limited spectrum of Fig. 3 ($T \simeq 20$ K) with a saturation contrast around 8%. The spectral feature is the average over 30 single Lamb-dip acquisitions. Then, a Lorentzian fit (continuous line) is carried out to extract the line-center frequency and the FWHM. In the lower panel, fit residuals are also shown, from which a SNR ≃ 30 is estimated for the Lamb-dip feature.

Lorentzian line shape yields a FWHM of $\Gamma(\mathcal{F}_{\mathrm{mol}} = 6, \mathcal{F}_{\mathrm{He}} = 6) = (820 \pm 40)$ kHz and a line center of $\nu_0(\mathcal{F}_{\mathrm{mol}} = 6, \mathcal{F}_{\mathrm{He}} = 6) = (196696652903 \pm 12)$ kHz. As discussed later, systematic uncertainties associated with the absolute determination of the line-center frequency are estimated well below our current statistical uncertainty level ($6 \cdot 10^{-11}$). Our ν_0 measurement is consistent with the value (196696652918 ± 2) kHz previously obtained at room temperature by Madej *et al.* with a dip-locked spectrometer [38]. Although several other room-temperature precision measurements have been performed more recently on C_2H_2 ro-vibrational lines [35,39,40], that work still holds the record of uncertainty on the line-center frequency, representing the top of a long course of spectroscopic research on acetylene as a secondary frequency standard. For this reason, the C_2H_2 molecule is an outstanding benchmark to assess the validity of our scheme at its early development stage. In this respect, our SCAR-BGC apparatus, susceptible to many improvements (see discussion at the end of this section), marks the beginning of a new, low-temperature generation of highly accurate spectroscopic frequency measurements on simple molecules. Additionally, our cryogenic experiment can be used to perform Lamb-dip spectroscopy of many complex molecules that are not good candidates for a room-temperature measurement.

Subsequently, for the same ro-vibrational line, Lamb-dip signals are recorded for different pairs $(\mathcal{F}_{\mathrm{mol}}, \mathcal{F}_{\mathrm{He}})$ of gaseous fluxes. For each sub-Doppler feature, a Lorentzian fit returns the line-center frequency and the FWHM along with their associated errors. Then, as shown in Fig. 5, the self-collisional broadening coefficient γ_{self} is determined by the slope of a linear fit to the FWHM values measured as a function of $\mathcal{F}_{\mathrm{mol}}$ (for a given $\mathcal{F}_{\mathrm{He}}$): $\gamma_{\mathrm{self}} = (60 \pm 20)$ kHz/SCCM. Likewise, as displayed in Fig. 6, the foreign collisional broadening coefficient $\gamma_{\mathrm{foreign}}$ is determined by the slope of a linear fit to the FWHM values measured as a function of $\mathcal{F}_{\mathrm{He}}$ (for a given $\mathcal{F}_{\mathrm{mol}}$): $\gamma_{\mathrm{foreign}} = (66 \pm 9)$ kHz/SCCM. For $\mathcal{F}_{\mathrm{mol}} = \mathcal{F}_{\mathrm{He}} = 6$ SCCM, the overall collisional broadening contribution is $\Gamma_{\mathrm{coll}} = \gamma_{\mathrm{self}}\mathcal{F}_{\mathrm{mol}} + \gamma_{\mathrm{foreign}}\mathcal{F}_{\mathrm{He}} = (760 \pm 170)$ kHz. The value found for γ_{self}, even compatible with zero, is consistent with the fact that, since the helium density in the buffer cell is much larger than that of acetylene, the rate of C_2H_2 – C_2H_2 collisions is expected to be far lower than that of C_2H_2 – He collisions. Concerning the absolute determination of the line-center frequency, limited by our statistical uncertainty level, the corresponding self and foreign collisional shift coefficients δ_{self} and $\delta_{\mathrm{foreign}}$ could not be retrieved with sufficient accuracy (see discussion below and the captions of Figs. 5 and 6).

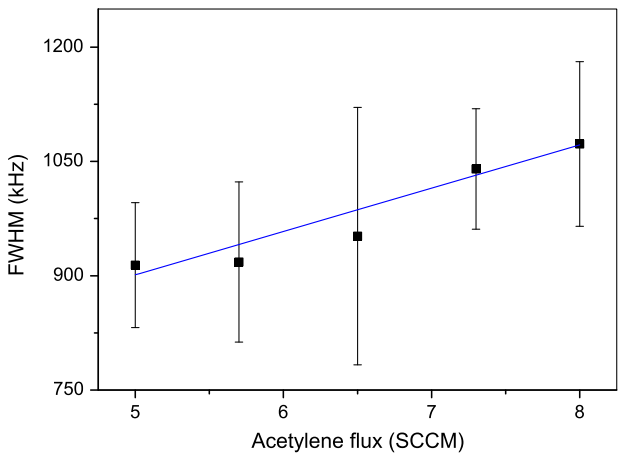

Fig. 5. FWHM of the observed Lamb-dip spectra as a function of the C_2H_2 flux injected into the BGC cell (for a given He flux, $\mathcal{F}_{\mathrm{He}} = 8$ SCCM). A linear fit to the data points extracts the self-collisional broadening coefficient: $\gamma_{\mathrm{self}} = (60 \pm 20)$ kHz/SCCM. As mentioned in the text, the corresponding self-collisional shift coefficient δ_{self} could not be significantly estimated (by the slope of a linear fit to the ν_0 values against $\mathcal{F}_{\mathrm{mol}}$): $\delta_{\mathrm{self}} = (-4 \pm 5)$ kHz/SCCM.

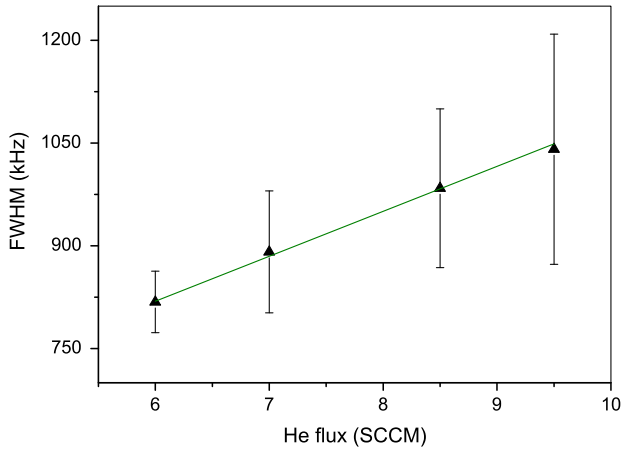

Fig. 6. FWHM of the observed Lamb-dip spectra versus the He flux injected into the BGC cell (for a given C_2H_2 flux, $\mathcal{F}_{\mathrm{mol}} = 6$ SCCM). A linear fit to the data points yields the foreign collisional broadening coefficient: $\gamma_{\mathrm{foreign}} = (66 \pm 9)$ kHz/SCCM. Also, in this case, the corresponding foreign collisional shift coefficient $\delta_{\mathrm{foreign}}$ could not be estimated with sufficient accuracy: $\delta_{\mathrm{foreign}} = (1 \pm 3)$ kHz/SCCM.

The saturation intensity I_{sat} of the investigated ro-vibrational transition is calculated according to $I_{\mathrm{sat}} = (3c\epsilon_0\hbar^2\Gamma_{\mathrm{obs}}^2)/(2\mu^2) \simeq 8.9$ W/cm^2 [41] using the transition dipole moment $\mu \simeq 0.67 \cdot 10^{-2}$ D provided by the HITRAN database [42] and taking the observed FWHM as $\Gamma_{\mathrm{obs}} \simeq 1$ MHz (here, ϵ_0 denotes the vacuum permittivity and $\hbar$ the reduced Planck constant). Then, denoting with $P \simeq 80$ mW the intracavity laser power, calculated dividing the power transmitted from the cavity by the experimental mirror transmission ($1.3 \cdot 10^{-5}$), the power broadening effect (of multiplicative type) is quantified as $\sqrt{1 + (P/\pi w_0^2) I_{\mathrm{sat}}^{-1}} \simeq 1.3$, with $w_0 = 700$ μm being the cavity mode waist. Finally, it may be useful to estimate, in our experimental conditions, also the transit-time broadening contribution (due to the finite interaction time of the molecules through the cross-sectional area of the probe laser beam): $\Gamma_{tt} = \sqrt{16 \ln 2/\pi^3}\sqrt{k_B T/m}\, w_0^{-1} = (68 \pm 5)$ kHz for $T = (20 \pm 3)$ K [43]. It should be noted that the above formula for the transit-time broadening refers to a single atom (or molecule) traveling with the mean thermal speed of the ensemble.

Table 1 quantifies the major sources of systematic uncertainty in the absolute measurement of the center frequency of the investigated $(\nu_1 + \nu_3)$ R(1) ro-vibrational line. Conservatively, the accuracy of the gas flow controllers (0.05 SCCM) used in the experiment translates into a contribution of $0.05 \cdot \Delta\delta_{\mathrm{self}} = 0.25$ kHz and $0.05 \cdot \Delta\delta_{\mathrm{foreign}} = 0.15$ kHz, respectively. The stability of the GPS-based frequency reference chain affects the line position over 900 s by about 0.2 kHz (calculated from the actual measured value of the Allan deviation). A 20% uncertainty on the

Table 1. Summary of Estimated Systematic Uncertainties Associated with the Absolute Determination of the Center Frequency of the $(\nu_1 + \nu_3)$ R(1) Ro-vibrational Line

Source of Systematic Shift	Estimated Uncertainty (kHz)
He flux measurement	0.15
C_2H_2	0.25
GPS-based reference chain	0.2
Intracavity power	<0.2
Lamb-dip fit	0.3
Total shift	**0.5**

intracavity power, as weighted with a power shift coefficient of −12 Hz/mW [38,44], gives a contribution below 0.2 kHz. Finally, by allowing the static width of the Lorentzian line shape to vary sigmoidally, an uncertainty contribution around 0.3 kHz is ascribed to asymmetries in the Lamb-dip fit [45].

In order to suppress collisional broadening effects and hence approach the transit-time-limited regime, the next step is to considerably reduce the gas flows entering the buffer cell. This implies, however, a further improvement in the detection sensitivity of the spectrometer. For this purpose, a new mechanical design for the enhancement cavity, where the mirror mounts are not connected directly to the vacuum vessel, is under construction in order to much more effectively break off vibrations from the PT cryo-cooler. In turn, this more stable optical resonator will enable the implementation of a high-bandwidth Pound–Drever–Hall scheme to lock the probe laser to the high-finesse cavity, leading to substantially increased ring-down event acquisition rates [46]. After that, acquiring the SCAR signal with a 24-bit (vertical resolution) digitizer will allow us, through the use of a more comprehensive fitting function [47], to better describe the time-dependent gas saturation level of the absorbing gas. This will make it possible to get rid of most fluctuations in the empty-cavity decay rate, also allowing much longer measurement times [48]. Enhancing the SNR of the Lamb-dip signals will also allow us to test fitting line-shape functions different from a Lorentzian in order to investigate low-temperature physical effects. Ultimately, this upgrade process in the experimental apparatus will result in the application of the SCAR technique shown here to the (collision-free) molecular beam emerging from the BGC cell.

4. CONCLUSION

In conclusion, we have established a new scheme for saturation sub-Doppler ro-vibrational spectroscopy of cold stable molecules. Thanks to the great versatility of both the BGC and the SCAR technique, the spectroscopic study reported here may be readily extended to plenty of molecular species, particularly of atmospheric [49] or astrophysical interest [50,51], in different spectral regions. This opens the door to extensive, accurate measurements of basic spectroscopic parameters in the range of a few Kelvin, and thus produces new sets of ultra-precise frequency measurements and provides an effective tool to probe fundamental low-temperature interaction processes [52]. Further developments can come from the implementation of other advanced interrogation schemes, like cavity-enhanced dual-comb spectroscopy [53]. Its combination with the present BGC setup could pave the way to sub-Doppler broadband multi-heterodyne spectroscopy of cold molecules, following the first demonstration of Doppler-free Fourier transform spectroscopy on an atomic system [54]. Cavity-enhanced two-photon excitation in the optical domain is another valuable option, having the additional advantage (compared to saturation sub-Doppler spectroscopy) that all the molecules contribute to the absorption, irrespective of their velocity, which results in a higher SNR [55]. Finally, given the enormous room for improvement, our system can be seen as the launchpad to high-accuracy molecular tests of fundamental physics at the electron volt energy scale. As an example, application of Lamb-dip spectroscopy to calculable molecules (H_2 and its isotopomers HeH^+ and metastable He_2) in the low-temperature regime could significantly improve the present accuracy in quantum electrodynamics (QED) tests [56,57]. Also, experiments probing parity violation in chiral molecules [58] or testing the time stability of the proton-to-electron mass ratio [9,10] would benefit enormously from the application of saturated-absorption laser spectroscopy to cold molecular samples.

Acknowledgment. The authors acknowledge fruitful discussions with G. Giusfredi and I. Galli.

REFERENCES

1. M. S. Safronova, D. Budker, D. DeMille, D. F. Jackson Kimball, A. Derevianko, and C. W. Clark, "Search for new physics with atoms and molecules," Rev. Mod. Phys. **90**, 025008 (2018).
2. A. D. Ludlow, M. M. Boyd, J. Ye, E. Peik, and P. O. Schmidt, "Optical atomic clocks," Rev. Modern Phys. **87**, 637–701 (2015).
3. T. E. Wall, "Preparation of cold molecules for high-precision measurements," J. Phys. B **49**, 243001 (2016).
4. R. K. Altmann, S. Galtier, L. S. Dreissen, and K. S. E. Eikema, "High-precision Ramsey-comb spectroscopy at deep ultraviolet wavelengths," Phys. Rev. Lett. **117**, 173201 (2016).
5. F. M. J. Cozijn, P. Dupre, E. J. Salumbides, K. S. E. Eikema, and W. Ubachs, "Sub-Doppler frequency metrology in HD for test of fundamental physics," Phys. Rev. Lett. **120**, 153002 (2018).
6. S. Alighanbari, M. G. Hansen, V. I. Korobov, and S. Schiller, "Rotational spectroscopy of cold and trapped molecular ions in the Lamb-Dicke regime," Nat. Phys. **14**, 555–559 (2018).
7. L. Santamaria, C. Braggio, G. Carugno, V. Di Sarno, P. Maddaloni, and G. Ruoso, "Axion dark matter detection by laser spectroscopy of ultracold molecular oxygen: a proposal," New J. Phys. **17**, 113025 (2015).
8. C. Braggio, G. Carugno, F. Chiossi, A. Di Lieto, M. Guarise, P. Maddaloni, A. Ortolan, G. Ruoso, L. Santamaria, J. Tasseva, and M. Tonelli, "Axion dark matter detection by laser induced fluorescence in rare-earth doped materials," Sci. Rep. **7**, 15168 (2017).
9. A. Shelkovnikov, R. J. Butcher, C. Chardonnet, and A. Amy-Klein, "Stability of the proton-to-electron mass ratio," Phys. Rev. Lett. **100**, 150801 (2008).
10. L. Santamaria, V. Di Sarno, I. Ricciardi, S. Mosca, M. De Rosa, G. Santambrogio, P. Maddaloni, and P. De Natale, "Assessing the time constancy of the proton-to-electron mass ratio by precision ro-vibrational spectroscopy of a cold molecular beam," J. Mol. Spectrosc. **300**, 116–123 (2015).
11. J. Baron, W. C. Campbell, D. DeMille, J. M. Doyle, G. Gabrielse, Y. V. Gurevich, P. W. Hess, N. R. Hutzler, E. Kirilov, I. Kozyryev, B. R. O'Leary, C. D. Panda, M. F. Parsons, E. S. Petrik, B. Spaun, A. C. Vutha, and A. D. West, "Order of magnitude smaller limit on the electric dipole moment of the electron," Science **343**, 269–272 (2013).
12. L. Anderegg, B. L. Augenbraun, Y. Bao, S. Burchesky, L. W. Cheuk, W. Ketterle, and J. M. Doyle, "Laser cooling of optically trapped molecules," Nat. Phys. **14**, 890–893 (2018).
13. H. J. Williams, L. Caldwell, N. J. Fitch, S. Truppe, J. Rodewald, E. A. Hinds, B. E. Sauer, and M. R. Tarbutt, "Magnetic trapping and coherent control of laser-cooled molecules," Phys. Rev. Lett. **120**, 163201 (2018).
14. J. D. Weinstein, R. deCarvalho, K. Amar, A. Boca, B. C. Odom, B. Friedrich, and J. M. Doyle, "Spectroscopy of buffer-gas cooled vanadium

monoxide in a magnetic trapping field," J. Chem. Phys. **109**, 2656–2661 (1998).
15. S. E. Maxwell, N. Brahms, R. deCarvalho, D. R. Glenn, J. S. Helton, S. V. Nguyen, D. Patterson, J. Petricka, D. DeMille, and J. M. Doyle, "High-flux beam source for cold, slow atoms or molecules," Phys. Rev. Lett. **95**, 173201 (2005).
16. J. K. Messer and F. C. De Lucia, "Measurement of pressure-broadening parameters for the CO-He system at 4 K," Phys. Rev. Lett. **53**, 2555–2558 (1984).
17. S. M. Skoff, R. J. Hendricks, C. D. J. Sinclair, M. R. Tarbutt, J. J. Hudson, D. M. Segal, B. E. Sauer, and E. A. Hinds, "Doppler-free laser spectroscopy of buffer-gas-cooled molecular radicals," New J. Phys. **11**, 123026 (2009).
18. D. Patterson and J. M. Doyle, "Cooling molecules in a cell for FTMW spectroscopy," Mol. Phys. **110**, 1757–1766 (2012).
19. L. Santamaria, V. Di Sarno, P. De Natale, M. De Rosa, M. Inguscio, S. Mosca, I. Ricciardi, D. Calonico, F. Levi, and P. Maddaloni, "Comb-assisted cavity ring-down spectroscopy of a buffer-gas-cooled molecular beam," Phys. Chem. Chem. Phys. **18**, 16715–16720 (2016).
20. B. Spaun, P. Bryan Changala, D. Patterson, B. J. Bjork, O. H. Heckl, J. M. Doyle, and J. Ye, "Continuous probing of cold complex molecules with infrared frequency comb spectroscopy," Nature **533**, 517–520 (2016).
21. S. K. Tokunaga, R. J. Hendricks, M. R. Tarbut, and B. Darquié, "High-resolution mid-infrared spectroscopy of buffer-gas-cooled methyltrioxorhenium molecules," New J. Phys. **19**, 053006 (2017).
22. G. Z. Iwata, R. L. McNally, and T. Zelevinsky, "High-resolution optical spectroscopy with a buffer-gas-cooled beam of BaH molecules," Phys. Rev. A **96**, 022509 (2017).
23. P. B. Changala, M. L. Weichman, K. F. Lee, M. E. Fermann, and J. Ye, "Rovibrational quantum state resolution of the C_{60} fullerene," Science **363**, 49–54 (2019).
24. O. Asvany, K. Yamada, S. Brünken, A. Potapov, and S. Schlemmer, "Experimental ground-state combination differences of CH_5^+," Science **347**, 1346–1349 (2015).
25. S. Lee, D. Hauser, O. Lakhmanskaya, S. Spieler, E. Endres, K. Geistlinger, S. Kumar, and R. Wester, "Terahertz-visible two-photon rotational spectroscopy of cold OD^-," Phys. Rev. A **93**, 032513 (2016).
26. G. Scoles, D. Bassi, U. Buck, and D. C. Laine, eds., *Atomic and Molecular Beam Methods* (Oxford University, 1988), Vol. **1**.
27. G. Scoles, D. C. Laine, and U. Valbusa, eds., *Atomic and Molecular Beam Methods* (Oxford University, 1992), Vol. **2**.
28. W. Demtröder, *Laser Spectroscopy*, Experimental Techniques (Springer, 2008), Vol. **2**.
29. D. Lisak and J. T. Hodges, "High-resolution cavity ring-down spectroscopy measurements of blended H_2O transitions," Appl. Phys. B **88**, 317–325 (2007).
30. G. Giusfredi, S. Bartalini, S. Borri, P. Cancio, I. Galli, D. Mazzotti, and P. De Natale, "Saturated-absorption cavity ring-down spectroscopy," Phys. Rev. Lett. **104**, 110801 (2010).
31. J. Burkart, T. Sala, D. Romanini, M. Marangoni, A. Campargue, and S. Kassi, "Communication: Saturated CO_2 absorption near 1.6 μm for kilohertz-accuracy transition frequencies," J. Chem. Phys. **142**, 191103 (2015).
32. I. Sadiek and G. Friedrichs, "Saturation dynamics and working limits of saturated absorption cavity ringdown spectroscopy," Phys. Chem. Chem. Phys. **18**, 22978–22989 (2016).
33. M. de Labachelerie, K. Nakagawa, Y. Awaji, and M. Ohtsu, "High-frequency-stability laser at 1.5 μm using Doppler-free molecular lines," Opt. Lett. **20**, 572–574 (1995).
34. V. Ahtee, M. Merimaa, and K. Nyholm, "Precision spectroscopy of acetylene transitions using an optical frequency synthesizer," Opt. Lett. **34**, 2619–2621 (2009).
35. D. Gatti, R. Gotti, A. Gambetta, M. Belmonte, G. Galzerano, P. Laporta, and M. Marangoni, "Comb-locked Lamb-dip spectrometer," Sci. Rep. **6**, 27183 (2016).
36. L. Santamaria, V. Di Sarno, I. Ricciardi, M. De Rosa, S. Mosca, G. Santambrogio, P. Maddaloni, and P. De Natale, "Low-temperature spectroscopy of the $^{12}C_2H_2(\nu_1+\nu_3)$ band in a helium buffer gas," Astrophys. J. **801**, 50 (2015).
37. V. Di Sarno, P. De Natale, J. Tasseva, L. Santamaria, E. Cané, F. Tamassia, and P. Maddaloni, "Frequency-comb-assisted absolute calibration and linestrength of $H^{12}C^{13}CH$ ro-vibrational transitions in the $2\nu_3$ band," J. Quantum Spectrosc. Radiat. Transfer **206**, 31–35 (2018).
38. A. A. Madej, A. J. Alcock, A. Czajkowski, J. E. Bernard, and S. Chepurov, "Accurate absolute reference frequencies from 1511 to 1545 nm of the $\nu_1+\nu_3$ band of $^{12}C_2H_2$ determined with laser frequency comb interval measurements," J. Opt. Soc. Am. B **23**, 2200–2208 (2006).
39. L.-G. Tao, T.-P. Hua, Y. R. Sun, J. Wang, A.-W. Liu, and S.-M. Hu, "Frequency metrology of the acetylene lines near 789 nm from Lamb-dip measurements," J. Quantum Spectrosc. Radiat. Transfer **210**, 111–115 (2018).
40. T.-P. Hua, Y. R. Sun, J. Wang, C.-L. Hu, L.-G. Tao, A.-W. Liu, and S.-M. Hu, "Cavity-enhanced saturation spectroscopy of molecules with sub-kHz accuracy," Chin. J. Chem. Phys. **32**, 1 (2019).
41. W. Ma, A. Foltynowicz, and O. Axner, "Theoretical description of Doppler-broadened noise-immune cavity-enhanced optical heterodyne molecular spectroscopy under optically saturated conditions," J. Opt. Soc. Am. B **25**, 1144–1155 (2008).
42. C. Hill, I. E. Gordon, R. V. Kochanov, L. Barrett, J. S. Wilzewski, and L. S. Rothman, "HITRAN-online: an online interface and the flexible representation of spectroscopic data in the HITRAN database, (http://hitran.org/)," J. Quantum Spectrosc. Radiat. Transfer 177, 4 (2016).
43. K. Shimoda, ed., *High-Resolution Laser Spectroscopy* (Springer-Verlag, 1976).
44. A. Czajkowski, A. A. Madej, and P. Dubé, "Development and study of a 1.5 μm optical frequency standard referenced to the P(16) saturated absorption line in the $\nu_1+\nu_3$ overtone band of $^{12}C_2H_2$," Opt. Commun. **234**, 259–268 (2004).
45. A. L. Stancik and E. B. Brauns, "A simple asymmetric lineshape for fitting infrared absorption spectra," Vib. Spectrosc. **47**, 66–69 (2008).
46. A. Cygan, D. Lisak, P. Maslowski, K. Bielska, S. Wojtewicz, J. Domyslawska, R. S. Trawinski, R. Ciurylo, H. Abe, and J. T. Hodges, "Pound-Drever-Hall-locked, frequency-stabilized cavity ring-down spectrometer," Rev. Sci. Instrum. **82**, 063107 (2011).
47. G. Giusfredi, I. Galli, D. Mazzotti, P. Cancio, and P. De Natale, "Theory of saturated-absorption cavity ring-down: radiocarbon dioxide detection, a case study," J. Opt. Soc. Am. B **32**, 2223–2237 (2015).
48. I. Galli, S. Bartalini, R. Ballerini, M. Barucci, P. Cancio, M. De Pas, G. Giusfredi, D. Mazzotti, N. Akikusa, and P. De Natale, "Spectroscopic detection of radiocarbon dioxide at parts-per-quadrillion sensitivity," Optica **3**, 385–388 (2016).
49. S. Reuter, J. S. Sousa, G. D. Stancu, and J.-P. H. van Helden, "Review on VUV to MIR absorption spectroscopy of atmospheric pressure plasma jets," Plasma Sources Sci. Technol. **24**, 054001 (2015).
50. P. S. Barklem and R. Collet, "Partition functions and equilibrium constants for diatomic molecules and atoms of astrophysical interest," Astron. Astrophys. **588**, A96 (2016).
51. A. S. Burrows, "Spectra as windows into exoplanet atmospheres," Proc. Natl. Acad. Sci. USA **111**, 12601–12609 (2014).
52. D. S. N. Parker, F. Zhang, Y. S. Kim, R. I. Kaiser, A. Landera, V. V. Kislov, A. M. Mebel, and A. G. G. M. Tielens, "Low temperature formation of naphthalene and its role in the synthesis of PAHs (polycyclic aromatic hydrocarbons) in the interstellar medium," Proc. Natl. Acad. Sci. USA **109**, 53–58 (2012).
53. B. Bernhardt, A. Ozawa, P. Jacquet, M. Jacquey, Y. Kobayashi, T. Udem, R. Holzwarth, G. Guelachvili, T. W. Hänsch, and N. Picqué, "Cavity-enhanced dual-comb spectroscopy," Nat. Phys. **4**, 55–57 (2009).
54. S. A. Meek, A. Hipke, G. Guelachvili, T. W. Hänsch, and N. Picqué, "Doppler-free Fourier transform spectroscopy," Opt. Lett. **43**, 162–165 (2018).
55. J. Karhu, M. Vainio, M. Metsälä, and L. Halonen, "Frequency comb assisted two-photon vibrational spectroscopy," Opt. Express **25**, 4688–4699 (2017).
56. P. Jansen, L. Semeria, L. Esteban Hofer, S. Scheidegger, J. A. Agner, H. Schmutz, and F. Merkt, "Precision spectroscopy in cold molecules: the lowest rotational interval of He_2^+ and metastable He_2," Phys. Rev. Lett. **115**, 133202 (2015).
57. L.-G. Tao, A.-W. Liu, K. Pachucki, J. Komasa, Y. R. Sun, J. Wang, and S.-M. Hu, "Toward a determination of the proton-electron mass ratio from the Lamb-dip measurement of HD," Phys. Rev. Lett. **120**, 153001 (2018).
58. S. K. Tokunaga, C. Stoeffler, F. Auguste, A. Shelkovnikov, C. Daussy, A. Amy-Klein, C. Chardonnet, and B. Darquié, "Probing weak force-induced parity violation by high-resolution mid-infrared molecular spectroscopy," Mol. Phys. **111**, 2363–2373 (2013).